

# Nonlinear Aeroelastic/Aeroservoelastic Modeling by Block-Oriented Identification

Dario H. Baldelli\*

ZONA Technology, Inc., Scottsdale, Arizona 85251

Richard Lind†

University of Florida, Gainesville, Florida 32611

and

Martin Brenner‡

NASA Dryden Flight Research Center, Edwards, California 93523

The investigation of aeroelastic/aeroservoelastic stability through flight testing is an essential part of aircraft certification. The stability boundary prediction is especially difficult when the instability is associated with nonlinearities in the dynamics. An approach is presented for the characterization of the nonlinear dynamics by noniterative identification algorithms. Two different block-oriented nonlinear models are considered to augment existing linear models with nonlinear operators derived by analyzing experimental data. Specifically, focus is placed on the identification of Hammerstein or Wiener block-oriented models from a  $N$ -point data record  $\{\bar{u}_k, \bar{y}_k\}_{k=1}^N$  of observed input–output measurements from an aeroelastic/aeroservoelastic system. Central in the identification of block-oriented models is the use of an a priori set of orthonormal bases tuned with the dynamics of the aeroelastic/aeroservoelastic system. In both cases, a method is proposed to generate the orthonormal bases that is based on the cascade of input-normal balanced state-space realizations of all-pass filters. Case studies with a simulated structurally nonlinear prototypical two-dimensional wing section and actual F/A-18 active aeroelastic wing ground vibration test data are presented.

## Nomenclature

$B_i(q)$	= orthonormal basis function
$b_i$	= unknown matrix parameters
$C$	= damping matrix
$e$	= error or unmodeled dynamic signal
$F$	= input matrix
$f(\cdot)$	= nonlinear operator
$G(q)$	= linear component of the block-oriented model
$g_i$	= known vector fields
$K$	= stiffness matrix
$L$	= linear operator
$M$	= mass matrix
$N(\cdot)$	= nonlinear component of the block-oriented model
$P$	= nominal plant
$q$	= forward shift operator
$s$	= number of Kautz filter
$\bar{u}$	= measured input signal
$w$	= input from nonlinear operator
$y$	= linear model output signal
$\bar{y}$	= measured output signal
$z$	= output to nonlinear operator
$\alpha_i$	= unknown matrix parameters

## Subscripts

$i$	= vector field index
$k$	= sample index
$l$	= orthonormal basis index

Received 25 June 2004; revision received 29 September 2004; accepted for publication 30 September 2004. Copyright © 2004 by Dario H. Baldelli. Published by the American Institute of Aeronautics and Astronautics, Inc., with permission. Copies of this paper may be made for personal or internal use, on condition that the copier pay the \$10.00 per-copy fee to the Copyright Clearance Center, Inc., 222 Rosewood Drive, Danvers, MA 01923; include the code 0731-5090/05 \$10.00 in correspondence with the CCC.

\*Control Engineering Specialist. Member AIAA.

†Assistant Professor, Department of Mechanical and Aerospace Engineering. Senior Member AIAA.

‡Aerospace Engineer, Code RS, Aerostructures Branch. Member AIAA.

## Introduction

INTENSE research has been observed recently in the field of nonlinear data-based modeling for aeroelastic/aeroservoelastic (AE/ASE) systems within the flight test community.<sup>1,2</sup> Some of the current generation fighter aircrafts carrying external stores tend to develop nonlinear oscillations of fixed frequency and amplitude, defined as limit-cycle oscillations (LCO), in the high subsonic to low supersonic airspeed regime.<sup>3,4</sup> Linear flutter engineering tools only are able to predict divergent oscillations, whereas the observed in flight dynamic behavior is of limited amplitude. Hence, some kind of nonlinear AE/ASE modeling capability must be developed to update production flutter analysis tools to explain in-flight observed nonlinear dynamic system behavior.

This work proposes the estimation of the observed nonlinear dynamics within an interconnected feedback framework, where the unknown dynamics turn out to be a function of the measured state vector  $x(t)$  and/or the measured input vector  $u(t)$  of the AE/ASE model. To this end, a class of nonlinear models called block-oriented, which consists of the interconnection of linear time invariant (LTI) systems and memoryless nonlinearities, is used. In particular, this paper focuses on the identification of Hammerstein, or Wiener, block-oriented models from an  $N$ -point data record of observed input–output measurements from an AE/ASE system.

The approach adopted here is motivated by Gómez and Baeyens.<sup>5</sup> The implemented identification algorithms are noniterative. These identification algorithms are composed of least square estimation (LSE) and singular value decomposition (SVD) stages. Specific identification strategies are formulated in accordance with the nature of the available data set. In general, actuator nonlinearities give rise to Hammerstein models, whereas output nonlinearities can be represented using Wiener models.

The focus of this work seeks to augment existing linear models with nonlinear operators derived by analyzing flight-test data. The analytical models developed by commercial packages, such as ZAERO,<sup>6</sup> are currently able to generate highly accurate representations of the linear dynamics, and so this information must be included. Thus, these models would be suitable for analyzing AE/ASE data if the unknown nonlinearities could be included. Moreover, if

the identified memoryless nonlinearity is an odd function, it can be replaced by its single input describing function (SIDF), and the resulting models could be used to compute robust stability margins using the  $\mu$  method to predict LCO.<sup>7</sup>

Promising results were obtained when this data-based modeling approach was applied to a structurally nonlinear two-dimensional wing section as well as to a set of F-18/AAW ground vibration test (GVT) data. The results indicate that this procedure reproduces, with a high degree of fidelity, the nonlinear dynamic system behavior present in the observed measurement set.

**Nonlinear AE/ASE Feedback System**

In Ref. 8, a general AE/ASE nonlinear linear fractional transformation (LFT) feedback setup for identification purposes is established. In particular, the proposed interconnected nonlinear feedback framework allows an expedient and efficient estimation of the unknown dynamics, or errors from flight data measurements. In the devised procedure, the unknown dynamics are denoted by the operator  $f(z)$  with  $z(t)$  being a function of the measured state vector  $\mathbf{x}(t)$  and/or the measured input vector  $\mathbf{u}(t)$  of the AE/ASE model.

Specific formulations were derived for two different unmodeled dynamic identification scenarios. One scenario assumes that the unknown dynamics are purely a function of the measured states  $f(z) = f(x)$ , whereas the other assumes that the unknown dynamics are purely a function of the measurement inputs  $f(z) = f(u)$ . In this paper, the former scenario is discussed; the latter was already considered in Ref. 9.

Let us consider the generalized AE/ASE equation of motion

$$M\ddot{\mathbf{x}} + C\dot{\mathbf{x}} + K\mathbf{x} - F\mathbf{u} = f(z) \tag{1}$$

where  $\mathbf{x}(t) \in \mathbb{R}^{n_x}$  and  $\mathbf{u}(t) \in \mathbb{R}^{n_u}$  are the state and input vectors and  $M \in \mathbb{R}^{n_x \times n_x}$ ,  $C \in \mathbb{R}^{n_x \times n_x}$ ,  $K \in \mathbb{R}^{n_x \times n_x}$ , and  $F \in \mathbb{R}^{n_x \times n_u}$  are the generalized mass, damping, stiffness and input matrices of the nominal AE/ASE system, respectively. The additional signal  $z(t) \in \mathbb{R}^{n_z}$  is dimensioned such that  $f : \mathbb{R}^{n_z} \rightarrow \mathbb{R}^{n_x}$  is in general a nonlinear mapping of appropriate dimension. As shown in Fig. 1, this model is now represented as a nonlinear data-sampled feedback LFT:

$$\bar{y}_k = F_l[P, f(z_k)]\bar{u}_k \tag{2}$$

$$P = \begin{bmatrix} P_{11} & P_{12} \\ P_{21} & P_{22} \end{bmatrix} \tag{3}$$

where  $P$  is the nominal plant and  $P_{ij}$ ,  $i, j = 1, 2$ , are the transfer functions related to the input  $\{\bar{u}_k^T \ w_k^T\}^T$  and output  $\{\bar{y}_k^T \ z_k^T\}^T$  signals. These transfer function matrices are built from the  $M$ ,  $C$ ,  $K$ , and  $F$  matrices of the nominal AE/ASE model. By LFT algebra, the known and unknown elements of the model are related through a feedback interconnection by the signal  $w_k = f(z_k)$ .

In what follows, the identification procedure focused on where the signal  $z_k$  is measured and can be inferred only from the knowledge of the measured output  $\bar{y}_k$ . This means that measurements at the input of the possible nonlinear dynamic system  $f(x_k)$  are accessible. Let us consider that the complete state vector  $\mathbf{x}_k$  is available from the measured output, that is,  $\mathbf{x}_k \equiv \bar{y}_k$ , then

$$\mathbf{x}_k = F_l[P, f(\mathbf{x}_k)]\bar{u}_k \tag{4}$$

Consequently, we can express the relationship as

$$\mathbf{x}_k = P_{11}\bar{u}_k + f(\mathbf{x}_k) \tag{5}$$

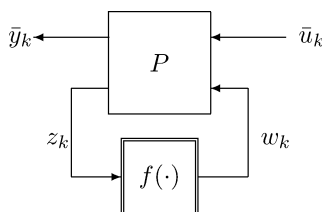


**Fig. 1 Generic nonlinear feedback framework.**

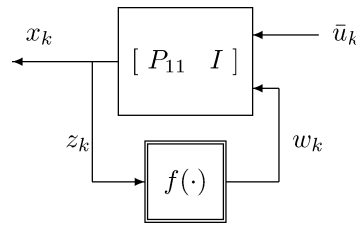


**Fig. 2 LFT with unmodeled dynamic  $f(x)$ .**

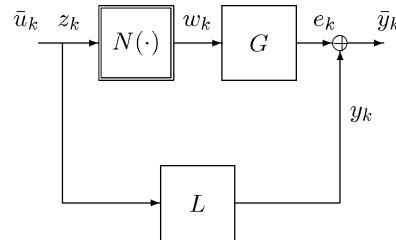


**Fig. 3 Nonlinear LFT modeling of  $\bar{y}_k$  with Hammerstein model.**

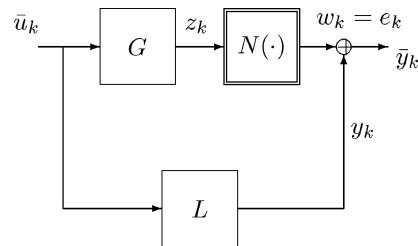


**Fig. 4 Nonlinear LFT modeling of  $\bar{y}_k$  with Wiener model.**

where  $P_{11}\bar{u}_k$  characterizes the linear component of the measured output signal  $\mathbf{x}_k$  and in addition it is assumed that  $P_{12} = I$ , as shown in Fig. 2. The key point is to visualize that the unmodeled dynamic system  $f(x_k)$  will give rise to a nonlinear operator that can be replaced with the Hammerstein,  $f(x_k) = GN(x_k)$ , or a Wiener,  $N(v_k)$ , model with the signal  $v_k = Gx_k$ , respectively. This model presents a clearly visible block structure of a memoryless nonlinear gain  $N(\cdot)$  and a LTI system  $G$  in cascade connection.

**Nonlinear Aeroelastic Feedback System by Using Block-Oriented Models**

The proposed interconnected nonlinear feedback model shown in Fig. 1 results in an extension of LFT models, and it can be used to model systems that exhibit limit cycles, subharmonics, nonlinear damping, and other nonlinear phenomena.<sup>10</sup>

In this section, we employ block-oriented models to augment existing linear models with nonlinear operators derived by analyzing experimental data. They consist of the interconnection of a LTI system with a memoryless nonlinearity. Several combinations of these two elements are possible, hence, giving rise to a set of different models. A model with a static nonlinearity at the input is called a Hammerstein model, and it can be associated with nonlinear actuators in the AE/ASE system. A Wiener model is defined if the static nonlinearity is located at the output, and this can be the case if the AE/ASE system has sensors with nonlinear behavior.

Figures 3 and 4 show the proposed AE/ASE model updating process. Then the nonlinear measured response  $\bar{y}_k$  is obtained as the result of adding the output  $y_k$  from the linear discrete-time model  $L(z_k)$ , with the error signal  $e_k$  coming from a Hammerstein or Wiener nonlinear model, respectively. Additionally, Figs. 3 and 4 show the input and output signals related with the nominal plant  $P$  and the nonlinearity  $f(\cdot)$  in the nonlinear LFT representation in Fig. 1. Specifically, the nominal plant  $P$ , associated with the Hammerstein and Wiener models are as follows.

Hammerstein:

$$P_H = \begin{bmatrix} L|G \\ I|0 \end{bmatrix}$$

Wiener:

$$P_W = \begin{bmatrix} L|I \\ G|0 \end{bmatrix}$$

Note that the signals  $z_k$  and  $w_k$  are incorporated to relate the nonlinearity to the nominal linear plant in a feedback interconnection. By closing the lower loop in Figs. 3 and 4, the input–output behavior of the proposed updated AE/ASE models are as follows:

For LFT with a Hammerstein model  $P_H$ ,

$$\bar{y}_k = F_l[P_H, N(z_k)]\bar{u}_k \quad (6)$$

$$\bar{y}_k = L\bar{u}_k + GN(\bar{u}_k) \quad (7)$$

For LFT with a Wiener model  $P_W$ ,

$$\bar{y}_k = F_l[P_W, N(z_k)]\bar{u}_k \quad (8)$$

$$\bar{y}_k = L\bar{u}_k + N(G\bar{u}_k) \quad (9)$$

In this way, the wind-tunnel or flight-test data can be used to update the linear flutter tool, represented by  $L$ , by using the proposed block-oriented nonlinear models.

### Block-Oriented Model Identification

It is assumed that nonlinearities in actuators and sensors can be represented by the interconnection of static nonlinearities and LTI systems. The outcome of the block-oriented identification problem will be the set of unknown parameters characterizing the nonlinear,  $N(\cdot)$ , and linear,  $G$ , blocks using the  $N$ -point data record  $\{\bar{u}_k, \bar{y}_k\}_{k=1}^N$  of input–output measurements.

The next two subsections closely follow the general identification framework developed by Gomez and Baeyens<sup>5</sup> for the estimation of block-oriented models using a set of orthonormal basis functions. In this work, the orthonormal basis set is generated from the cascade connection of two-parameters Kautz filters (see Ref. 11) tuned with the modal parameters contained in the measurements set  $\{\bar{u}_k, \bar{y}_k\}_{k=1}^N$ .

#### Hammerstein Model Identification

Consider the multivariable Hammerstein nonlinear model shown in Fig. 5. The model consists of a static nonlinearity in series connection with an LTI system. The nonlinear operator is

$$N(\bar{u}_k) = \sum_{i=1}^r \alpha_i \mathbf{g}_i(\bar{u}_k) \quad (10)$$

where  $\mathbf{g}_i \in \mathbb{R}^n \rightarrow \mathbb{R}^n$ ,  $i = 1, \dots, r$ , are vector fields chosen by the designer, and  $\alpha_i \in \mathbb{R}^{m \times n}$ ,  $i = 1, \dots, r$ , are the unknown matrix parameters to be estimated. The LTI system is described by its transfer function matrix,

$$G(q) = \sum_{l=0}^{p-1} b_l B_l(q) \quad (11)$$

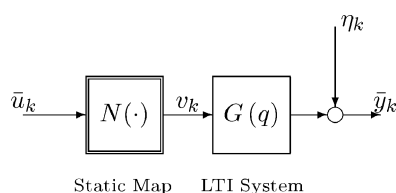


Fig. 5 Hammerstein model.

where  $G(q) \in \mathbb{H}_2^{m \times n}(\mathbb{T})$ ,  $\mathbb{T}$  is the unit circle,  $q$  is the forward shift operator,  $b_l \in \mathbb{R}^{m \times n}$  are unknown matrix parameters, and  $\{B_l q\}_{l=0}^{p-1}$  is the set of orthonormal basis. The input–output relationship, shown in Fig. 5, is then given by

$$\bar{y}_k = G(q)N(\bar{u}_k) + \eta_k \quad (12)$$

where  $\bar{y}_k \in \mathbb{R}^m$ ,  $\bar{u}_k \in \mathbb{R}^n$ , and  $\eta_k \in \mathbb{R}^m$  represent the system output, input, and measurement noise vectors at time  $k$ , respectively. When Eqs. (10) and (11) are substitute into Eq. (12), the input–output relationship is written as

$$\bar{y}_k = \sum_{l=0}^{p-1} \sum_{i=1}^r b_l \alpha_i B_l(q) \mathbf{g}_i(\bar{u}_k) + \eta_k \quad (13)$$

A unique parameterization is obtained if the parameter matrices  $\alpha_i$  are normalized, that is,  $\|\alpha_i\|_2 = 1$ . Lets now define

$$\theta \triangleq [b_0 \alpha_1, \dots, b_0 \alpha_r, \dots, b_{p-1} \alpha_1, \dots, b_{p-1} \alpha_r]^T \quad (14)$$

$$\phi_k \triangleq [B_0(q) \mathbf{g}_1^T(\bar{y}_k), \dots, B_0(q) \mathbf{g}_r^T(\bar{y}_k), \dots, B_{p-1}(q) \mathbf{g}_1^T(\bar{u}_k), \dots, B_{p-1}(q) \mathbf{g}_r^T(\bar{u}_k)]^T \quad (15)$$

When Eqs. (14) and (15) are placed into Eq. (13), the latter results in the regression vector

$$\bar{y}_k = \theta^T \phi_k + \eta_k \quad (16)$$

Now, with the data set  $\{\bar{u}_k, \bar{y}_k\}_{k=1}^N$  and defining the matrices  $Y_N \triangleq [\bar{y}_1^T, \dots, \bar{y}_N^T]$ ,  $\Gamma_N \triangleq [\eta_1^T, \dots, \eta_N^T]$  and  $\Phi_N \triangleq [\phi_1, \dots, \phi_N]$ , we obtain

$$Y_N = \Phi_N^T \theta + \Gamma_N \quad (17)$$

Consequently, by the least-squares criterion, an estimate  $\hat{\theta}$  of  $\theta$  can be computed. When  $\Theta_{ab}$  is defined as

$$\Theta_{ab} \triangleq \begin{bmatrix} \alpha_1^T b_0^T & \dots & \alpha_1^T b_{p-1}^T \\ \vdots & \dots & \vdots \\ \alpha_r^T b_0^T & \dots & \alpha_r^T b_{p-1}^T \end{bmatrix} = \alpha \mathbf{b}^T \quad (18)$$

with  $\alpha \triangleq [\alpha_1, \dots, \alpha_r]^T$  and  $\mathbf{b} \triangleq [b_0^T, \dots, b_{p-1}^T]$ , the parameter matrix can be expressed as  $\theta = \text{blockvec}(\Theta_{ab})$  (Ref. 12). Therefore, an estimate of  $\hat{\alpha}$  and  $\hat{\mathbf{b}}$  is obtained from the SVD of  $\hat{\Theta}_{ab}$  (Ref. 5).

#### Wiener Model Identification

A block scheme of a process with output nonlinearity in input–output representation is shown in Fig. 6, and it can be considered as a special case of the Volterra series. In Fig. 6,  $\bar{y}_k \in \mathbb{R}^m$ ,  $\bar{u}_k \in \mathbb{R}^n$ , and  $\eta_k \in \mathbb{R}^m$  are the system output, input, and process noise vectors at time  $k$ , respectively.

Let us now consider the multivariable feedback nonlinear model which consists of an LTI system described by Eq. (11). The nonlinear function  $N(\cdot) : \mathbb{R}^m \rightarrow \mathbb{R}^m$  is assumed to be invertible and given by

$$N^{-1}(\bar{y}_k) = \sum_{i=1}^r \alpha_i \mathbf{g}_i(\bar{y}_k) \quad (19)$$

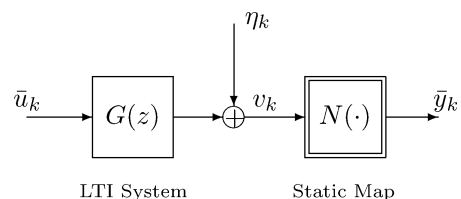


Fig. 6 Wiener model.

with  $\mathbf{g}_i(\cdot) : \mathbb{R}^m \rightarrow \mathbb{R}^m$ ,  $i = 1, \dots, r$ , the assumed vector fields that typically turn out to be a polynomial and  $\alpha_i \in \mathbb{R}^{m \times m}$ ,  $i = 1, \dots, r$ , the unknown matrix parameters. In what follows, it will be assumed that  $a_1 = I_m$ . In Fig. 6, the intermediate variable  $v_k$  can be written as

$$v_k = G(q)\bar{\mathbf{u}}_k + \boldsymbol{\eta}_k \quad (20)$$

In addition, it can be expressed as

$$v_k = N^{-1}(\bar{\mathbf{y}}_k) \quad (21)$$

When the right-hand sides of the two preceding equations are made equal and the parameterizations given by Eqs. (11) and (19) are considered,

$$\mathbf{g}_1(\bar{\mathbf{y}}_k) = -\sum_{i=2}^r \alpha_i \mathbf{g}_i(\bar{\mathbf{y}}_k) + \sum_{l=0}^{p-1} b_l B_l(q)\bar{\mathbf{u}}_k + \boldsymbol{\eta}_k \quad (22)$$

Let us define

$$\boldsymbol{\theta} \triangleq [\alpha_2, \alpha_3, \dots, \alpha_r, b_0, b_1, \dots, b_{p-1}]^T \quad (23)$$

$$\boldsymbol{\phi}_k \triangleq [-\mathbf{g}_2^T(\bar{\mathbf{y}}_k), -\mathbf{g}_3^T(\bar{\mathbf{y}}_k), \dots, -\mathbf{g}_r^T(\bar{\mathbf{y}}_k),$$

$$B_0(q)\bar{\mathbf{u}}_k^T, \dots, B_{p-1}(q)\bar{\mathbf{u}}_k^T]^T \quad (24)$$

It is clear that the vector  $\mathbf{g}_1(\bar{\mathbf{y}}_k)$  noted by Eq. (22) can be written in linear regression vector form as

$$\mathbf{g}_1(\bar{\mathbf{y}}_k) = \boldsymbol{\theta}^T \boldsymbol{\phi}_k + \boldsymbol{\eta}_k \quad (25)$$

By considering the  $N$ -point data set  $\{\bar{\mathbf{u}}_k, \bar{\mathbf{y}}_k\}_{k=1}^N$  and building the unknown and data-based matrices

$$Y_N = [\mathbf{g}_1(\bar{\mathbf{y}}_1)^T, \dots, \mathbf{g}_1(\bar{\mathbf{y}}_N)^T]^T, \quad \Gamma_N = [\boldsymbol{\eta}_1^T, \dots, \boldsymbol{\eta}_N^T]^T$$

$$\Phi_N = [\boldsymbol{\phi}_1^T, \dots, \boldsymbol{\phi}_N^T]^T$$

we obtain

$$Y_N = \Phi_N^T \boldsymbol{\theta} + \Gamma_N \quad (26)$$

When the least-squares criterion is used, an estimate  $\hat{\boldsymbol{\theta}}$  of  $\boldsymbol{\theta}$  is obtained as

$$\hat{\boldsymbol{\theta}} = (\Phi_N \Phi_N^T)^{-1} \Phi_N Y_N = \Phi_N^\dagger Y_N \quad (27)$$

Finally, the estimates parameters  $\hat{\alpha}_i$ ,  $i = 2, \dots, r$ , and  $\hat{b}_l$ ,  $l = 0, \dots, p - 1$ , result from the proper partition of  $\hat{\boldsymbol{\theta}}$  in Eq. (27), in accordance to its own definition in Eq. (23).

### Orthonormal Function Set Generation and Modal Parameter Estimation

Central in the identification of the preceding block-oriented models is the use of the a priori set of orthonormal bases  $\{B_l(q)\}_{l=0}^{p-1}$ . In this section, we propose a technique to tune the LTI part in the block-oriented model framework with the dynamic being defined using modal parameters of the linear model  $P_{11}$ , using a high-fidelity software package such as ZAERO,<sup>6</sup> or from some identified modal dynamics using the  $N$ -point data set  $\{\bar{\mathbf{u}}_k, \bar{\mathbf{y}}_k\}_{k=1}^N$ .

Because the focus is on the identification of AE/ASE structures, it is suggested to make broad use of the two-parameter Kautz filters to generate the set of basis functions (see Ref. 11). The Kautz filter's minimal realization is defined as  $H_i(z) = C_i(zI - A_i)^{-1}B_i + D_i$ , with the eigenvalues of  $A_j$  lying inside the unit circle. Also, a filter is all-pass if  $H_i(z)H_i(z^{-1}) = 1$ , and it is said to be orthonormal if its state-space realization  $(A_i, B_i, C_i, D_i)$  is input normal. In addition, a stable realization is input normal if  $W_c$  and  $W_0$  are defined as the solution of the following Lyapunov equations:

$$A_i W_c A_i^* - B_i B_i^* = W_c \quad (28)$$

$$A_i^* W_0 A_i - C_i^* C_i = W_0 \quad (29)$$

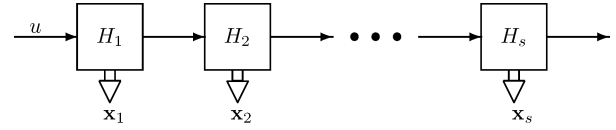


Fig. 7 Series connection of two-parameter Kautz filters.

where  $W_c = I$  and  $W_0 = \Sigma^2$ , with  $\Sigma = \text{diag}(\sigma_1, \dots, \sigma_{n_i})$ , and the decreasingly ordered scalar  $\sigma_1 \geq \dots \geq \sigma_{n_i} \geq 0$  are the Hankel singular values. Let  $H_{\text{Kautz}}(b, c)$  be

$$H_{\text{Kautz}}(b, c) = \frac{-cz^2 + b(c-1)z + 1}{z^2 + b(c-1)z - c} \quad (30)$$

with  $|b| < 1$  and  $|c| < 1$ , respectively. Thereby, it is possible to build a set of orthonormal basis functions from a family of stable all-pass filters with input normal realizations as shown in Fig. 7, that is,

$$H(z) = \prod_{j=1}^s H_j(z) \quad (31)$$

whose state-space input normal realization results

$$H(z) = C_n(zI - A)^{-1}B_n + D_n \quad (32)$$

with

$$n = \sum_{j=1}^s n_j$$

Now, let  $\mathbf{x} = (x_0^T, \dots, x_s^T)^T$  be the state of the filter  $H(z)$ , where each component  $x_j$  adopts the form  $\mathbf{x}_j = (x_{j1}, \dots, x_{jn_j})^T$ , for  $j = 1, \dots, s$ . Hence, the set of orthonormal basis are defined by the transfer function  $B_k(q)$  from the filter input  $u$  to each of the filter state components  $\mathbf{x}_k$ ,  $k = 0, \dots, p - 1$ ,

$$\mathbf{x}_k = B_k(q)u, \quad B_k(q) = \mathbf{c}_k(zI - A_n)^{-1}B_n \quad (33)$$

where  $\mathbf{c}_k$  is the  $k$ th Euclidean basis vector in  $\mathbb{R}^n$ .

Accordingly, the set of a priori basis functions used to describe the linear block  $G(q)$  can be tuned with the linear modal parameters contained in the high-fidelity linear model  $P_{11} = L$ , or from the a posteriori experimental evidence, such as wind-tunnel, GVT, or flight-test data of the AE/ASE system.

### Nonlinear AE/ASE Identification Examples

The approach proposed in this work will be applied to two case studies. The first involves simulated data, corrupted with noise, from a structurally nonlinear prototypical two-dimensional wing section, and it will be used to demonstrate the Hammerstein block-oriented model identification procedure. This easy-to-handle example is chosen to demonstrate the methodology against previous published results.<sup>8</sup>

The second case study involves experimental measurements from the F/A-18 active AE wing (AAW) GVT in the vertical plane and represents a highly complex ASE system. These examples will illustrate the use of the proposed block-oriented identification framework in practical situations.

#### Case Study 1: Nonlinear Pitch-Plunge AE System

The selected case is a structurally nonlinear prototypical two-dimensional wing section. The nonlinearity included in the model is a memoryless quadratic gain affecting the stiffness of the pitch motion through the pitch rotation of the airfoil ( $k_{\alpha 2} \alpha^2$ ). The system parameters to be used in the numerical simulations are given in Table 1 and the geometry of the aeroelastic model is the same as that considered in Ref. 13. In addition, the aeroelastic system matrices  $M$ ,  $K$ ,  $C$ , and  $F$  are identical to those presented in Ref. 8.

In this case, the simulated measured system output is the pitch angle  $\alpha(t)$ , which is corrupted with a zero-mean Gaussian distributed

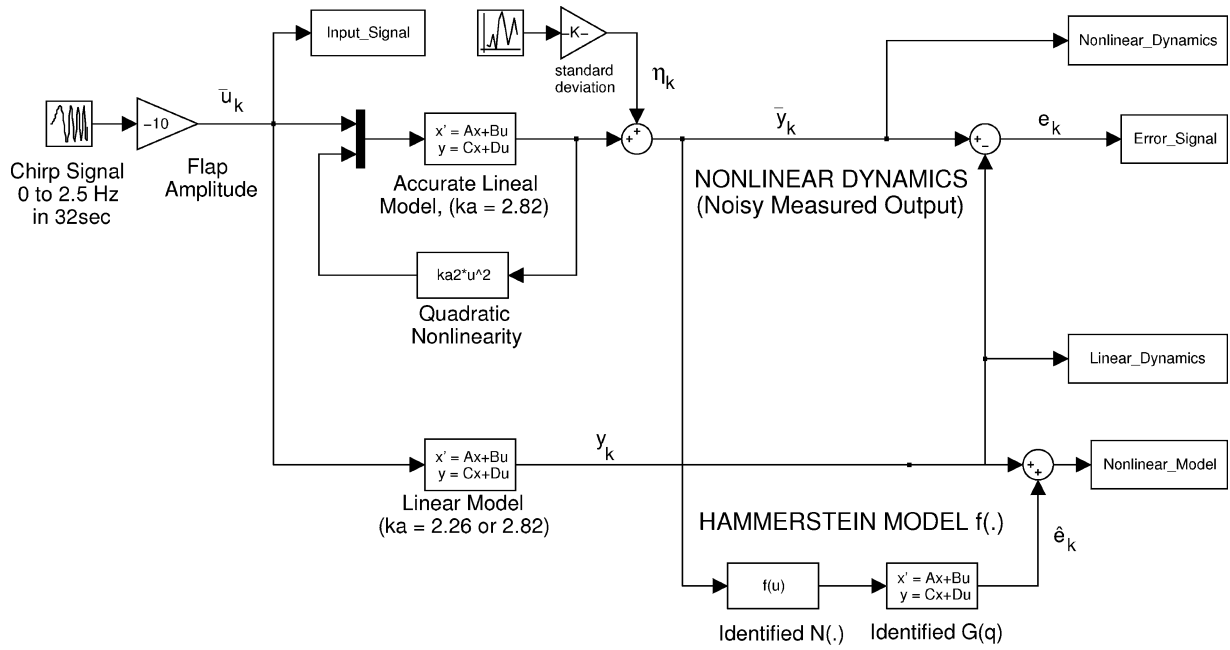


Fig. 8 Flowchart for  $X(\cdot)$  estimation.

Table 1 Aeroelastic system variables

Parameter	Value
$U$	6 m/s
$b$	0.135 m
$m$	12.387 m/s
$I_\alpha$	0.065 m <sup>2</sup> kg
$c_\alpha$	0.180 m <sup>2</sup> kg/s
$c_{I_\alpha}$	$2\pi$
$c_{I_\beta}$	3.358
$k_\alpha$	2.82 (accurate)
$k_\alpha$	2.26 (inaccurate)
$a$	-0.6
$\rho$	1.225 kg/m <sup>3</sup>
$x_\alpha$	0.2466
$k_h$	2844.4 N/m
$c_h$	27.43 kg/s
$c_{m_\alpha}$	-0.628
$c_{m_\beta}$	-0.635
$k_{\alpha^2}$	14.1

white noise with standard deviation  $\sigma = 0.01$ , and the system input is the flap deflection  $\beta(t)$ . In what follows, a noisy error signal  $e_k$  is defined as the difference between the measured signal  $\bar{y}_k$  (nonlinear dynamics) and the simulated linear part of the model,  $y_k = P_{11}\bar{u}_k$ . The Hammerstein nonlinear identification algorithm is employed to identify the unmodeled dynamics, from an  $N$ -point data of the noisy error signal  $e_k$  using a sampling frequency of 1000 Hz. In connection with the linear portion of the model,  $P_{11}$ , an explicit modeling error is incorporated by an inaccurate value of the pitch stiffness  $k_\alpha$ . Therefore, an accurate linear model results when the nominal pitch stiffness equal to  $k_\alpha = 2.82$  is used, whereas the inaccurate linear model is defined by  $k_\alpha = 2.26$ .

Figure 8 shows the flowchart model used to generate the simulated pitch deflection signal  $\bar{y}_k \equiv \alpha_k$  (nonlinear dynamics), as well as the response from the linear model. It is clearly visible that the signal used to drive the Hammerstein model  $f(\cdot)$  is the measured pitch  $\alpha_k$  and that the output of this system is the unmodeled dynamics or error estimation  $\hat{e}_k$  of  $e_k$ . The linear model used in this case is an inaccurate one, that is,  $k_\alpha = 2.26$ , and its output is denoted by  $y_k$ . The nonlinear model response is finally obtained when the estimation error  $\hat{e}_k$  is added to  $y_k$ . Additionally, all simulation data needed in the nonlinear identification algorithm are saved through the denoted variables within the boxes. Figure 9a shows the noisy nonlinear dynamic system signal  $\bar{y}_k$ , solid line, al-

together with the response of the inaccurate linear model  $y_k$ , dotted line.

The difference between both signals,  $e_k = \bar{y}_k - y_k$ , is plotted as a solid line in Fig. 9b. From the dynamics of  $P_{11}$ , two all-pass Kautz filters are used to generate the required four basis function set,  $\{B_k(q)\}_{k=0}^3$ . These are

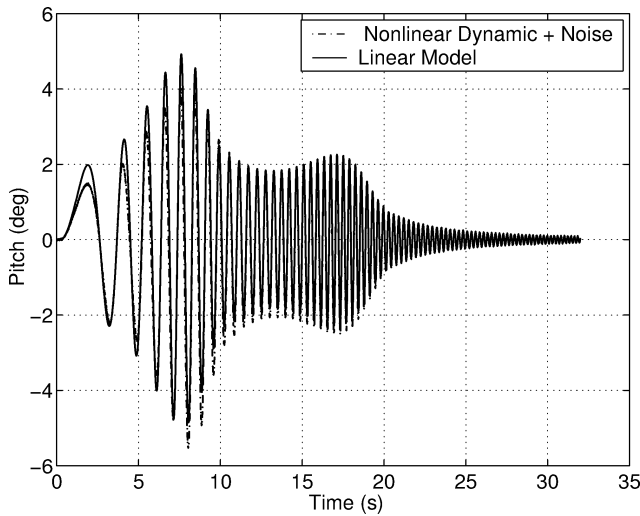
$$B_k(q) = \begin{bmatrix} 0.9998 & 0.0166 & 0 & 0 & 0 \\ -0.0166 & 0.9964 & 0 & 0 & 0.0831 \\ 0 & 0 & 0.9999 & 0.0067 & 0 \\ 0.0001 & 0.0065 & -0.0067 & 0.9969 & 0.0781 \\ \hline & & c_k & & 0 \end{bmatrix} \quad (34)$$

where  $c_k = [0 \ 1 \ 0 \ 0]$  is obtained by including a 1 in position  $k$  ( $k$ th Euclidean basis vector in  $\mathbb{R}^4$ ).

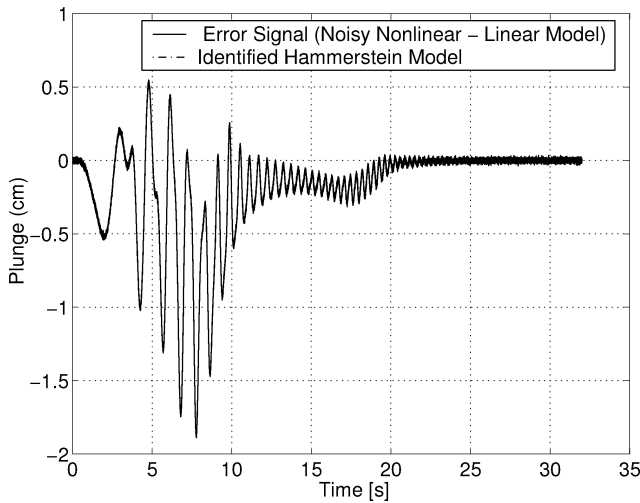
The Hammerstein model identification algorithm is now used to compute the unknown parameter vectors  $\hat{\alpha}$  and  $\hat{b}$  defined in Eq. (18). The estimated  $\hat{b}_k$  coefficients for this case are  $\hat{b}_0 = 3.048 \times 10^{-3}$ ,  $\hat{b}_1 = -2.6553 \times 10^{-3}$ ,  $\hat{b}_2 = 1.7607 \times 10^{-3}$ , and  $\hat{b}_3 = 2.9988 \times 10^{-3}$ , respectively. The dotted line in Fig. 9b shows the time trace of the output signal coming from the identified Hammerstein model  $\hat{f}(\cdot)$ . A good agreement between  $e_k$  and  $\hat{e}_k$  is obtained because it is almost impossible to distinguish one from the other.

The identified quadratic map  $\hat{N}(\cdot)$  is shown in Fig. 9c, and its identified coefficients are  $\hat{\alpha}_1 = -0.9155$  and  $\hat{\alpha}_2 = -0.4022$ . It is conjectured that the effects of using an inaccurate linear model  $P_{11}$  results in a noticeable displacement of the nonlinear map's origin from zero toward the left-hand plane. Therefore, the origin's displacement can be easily explained in terms of the magnitude of the estimate coefficient  $\hat{\alpha}_1$ . The large magnitude of it clearly indicates that the assumed linear model  $P_{11}$  is a poor representation of the true linear dynamics. Note that, when an accurate linear model  $k_\alpha = 2.82$  is used to estimate the noisy error dynamics  $e_k$ , the computed coefficients are  $\hat{\alpha}_1 = -0.0017$  ( $\hat{\alpha}_1 = 0$  when  $\bar{y}_k$  is an uncorrupted signal) and  $\hat{\alpha}_2 = -1$ . In other words, the estimated memoryless operator is presumably trying to cover the undermodeling linear model  $P_{11}$  with a strong linear term coefficient  $\hat{\alpha}_1$ .

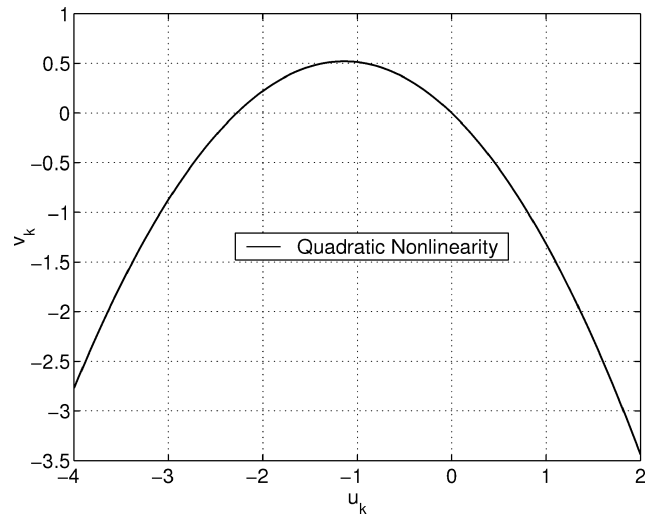
Finally, in Fig. 9d, the solid line is the time trace of the noisy simulated pitch response  $\bar{y}_k$ , and the dotted line is the output from the identified Hammerstein model  $y_k$ . Note that, besides the inaccurate linear model used to generate the basis function set  $\{B_k(q)\}_{k=0}^3$ , the nonlinear identification approach is able to reproduce with high fidelity the nonlinear behavior embedded in the output data  $\bar{y}_k$ .



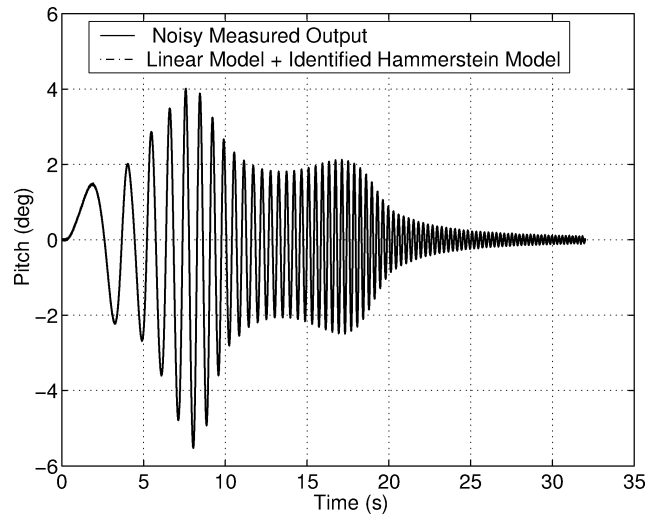
a) Response of noisy nonlinear dynamics  $\bar{y}_k$  and inaccurate linear system  $y_k$



b) Difference in measurements from noisy nonlinear dynamics and inaccurate linear model; blue,  $e_k = \bar{y}_k - y_k$  and red,  $\hat{e}_k$



c) Identified quadratic nonlinearity,  $N(u_k) = -0.9155 u_k - 0.4022 u_k^2$



d) Response of noisy nonlinear dynamics  $\bar{y}_k$  and nonlinear model  $y_k + \hat{e}_k$

Fig. 9 Pitch-plunge AE system.

### Case Study 2: F/A-18 AAW GVT Data Analysis

GVT were performed on the F/A-18 AAW aircraft to assess the structural characteristics of the modified airframe during the phase 1 flight research.<sup>14</sup> This subsection deals with the case of the F/A-18 AAW-ASE LTI model update by incorporating the unmodeled dynamics by using a Wiener model computed from the acceleration error signal. This signal is defined as the difference between the measured GVT data,  $n_{z,100}$ , and the predicted response coming from the ASE LTI model,  $N_z$ .

Vertical accelerometer data sampled at 100 Hz, that is,  $n_{z,100}$ , is recorded when the collective aileron  $c_{ail}$  performs a sinusoidal sweeps in the range 3–35 Hz over 35 s. Available data records last for 35 s, where the excitation software waits 5 s, and then begins the multi-sinusoidal commands. The commands continue for 25 s and then stops. Thereby, the first 5 s of GVT data are neglected, whereas the last 5 s are preserved given that they can be considered as actual free-decay data of the F/A-18 AAW aircraft.

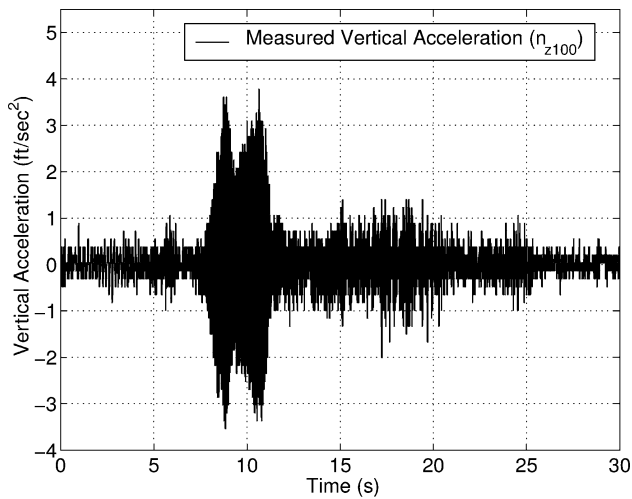
As in the earlier example, the ASE model update process is represented as a nonlinear feedback LFT between the nominal ASE model denoted by  $P$  and the unmodeled dynamic,  $f(\cdot)$ , as in Fig. 2. The latter will be replaced by the estimated block-oriented Wiener model.

Figure 10a shows the measured acceleration response,  $n_{z,100}$ , and Fig. 10b shows the ASE model response  $N_z$ . The unmodeled vertical

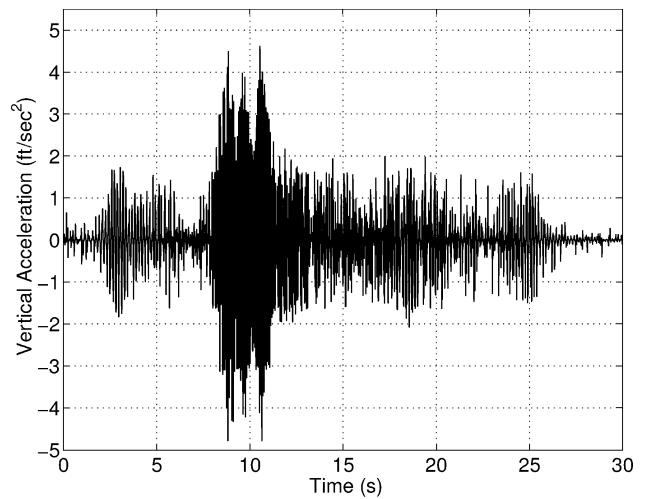
dynamic used to estimate the Wiener model is computed from these time traces as shown in Fig. 10c.

The set of basis functions  $\{B_l(q)\}_{l=0}^p$  used to describe the LTI block  $G(q)$  in Eq. (11) is tuned with the linear modal parameters contained in the  $N$ -data record of experimental evidence  $n_{z,100}$ . To this end, a multistage exogenous autoregressive moving average (ARMAX) procedure is applied. This technique is based on the coefficients of the ARMAX model that satisfy the maximum of the likelihood function corresponding to the experimental evidence. The first stage of the numerical algorithm involves the estimation of an exogenous autoregressive model (ARX) with more coefficients than required. This is because in practical situations the actual number of observable natural frequencies embedded in the frequency spectrum of the  $n_{z,100}$  signal is actually unknown. In the second stage, the coefficients of the ARMAX model are computed iteratively from the ARX coefficients. For further technical details about the multistage ARMAX approach, see Ref. 15.

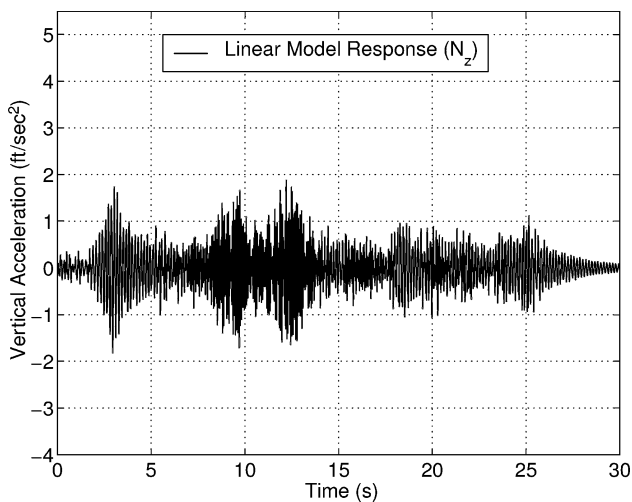
Therefore, there are six natural frequencies and damping ratios computed from the vertical GVT data, by using an ARMAX (22,21,22) model in the multistage process with an initial ARX model of order 60, as presented in Table 2. These modal parameters are used to tune the dynamics of the a priori set of orthonormal basis functions  $\{B_l(q)\}_{l=0}^5$  built through a series connection of two-parameter Kautz filters [Eq. (30)]. Note that there are many other



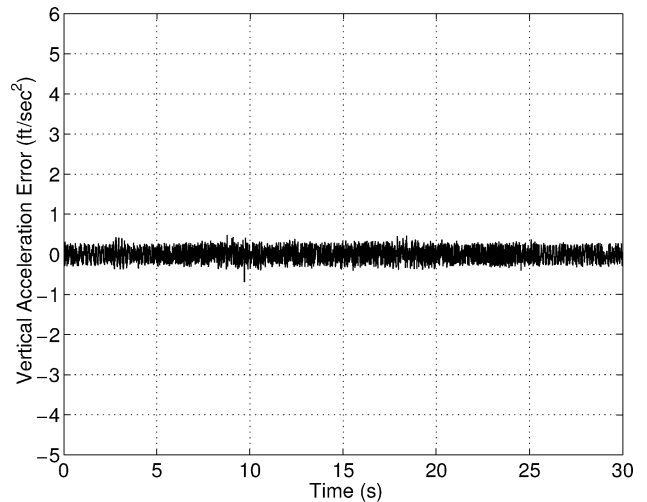
a) GVT measured vertical acceleration



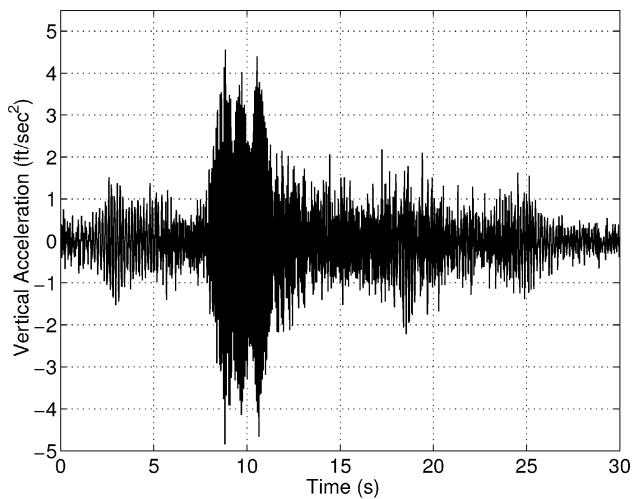
d) Identified vertical unmodeled acceleration



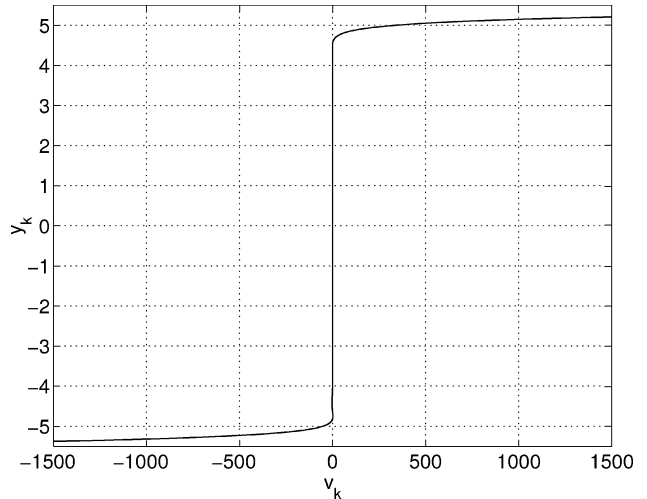
b) Analytical ASE linear vertical acceleration



e) Vertical acceleration error signal



c) Vertical unmodeled acceleration



f) Identified vertical dynamic staticmap (rate-limited type)

Fig. 10 F-18 AAW/GVT vertical acceleration data.

methods of modal parameters estimation to tuned the orthonormal function set,<sup>16,17</sup> the choice is up to the designer's preference; there is no restriction to any particular method.

The predicted response from the Wiener model is shown in Fig. 10d and is shown to compare quite closely with the unmodeled vertical signal shown in Fig. 10c. The identified Wiener model is built with a LTI block of order 12, using the natural frequencies and damping ratios shown in Table 2, followed by a polynomial

nonlinearity of order 17. The identification error is in Fig. 10e, and its behavior is assumed to be linked with the measurement noise present in the GVT data. Figure 10f shows the identified memoryless nonlinearity from the 17th-order polynomial. This nonlinearity shape closely resembles actuator rate-limited effects.

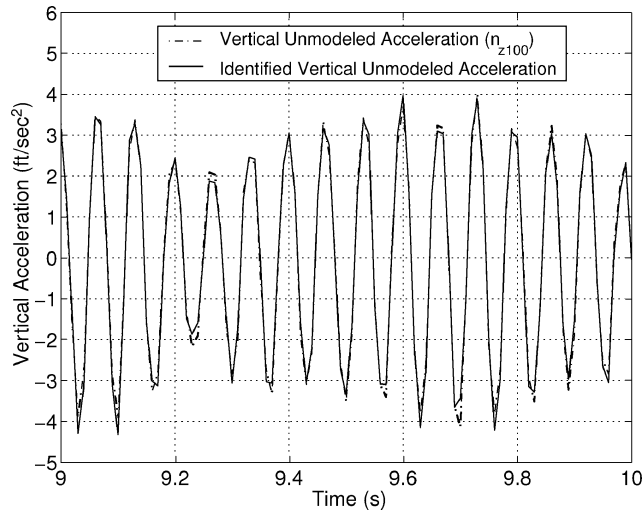
Figure 11 presents the predicted nonlinear response compared to the vertical unmodeled dynamic between 9 and 10 s. Figure 11a shows that a good match is obtained between prediction and

unmodeled dynamics. Minor differences are explicitly shown in Fig. 11b.

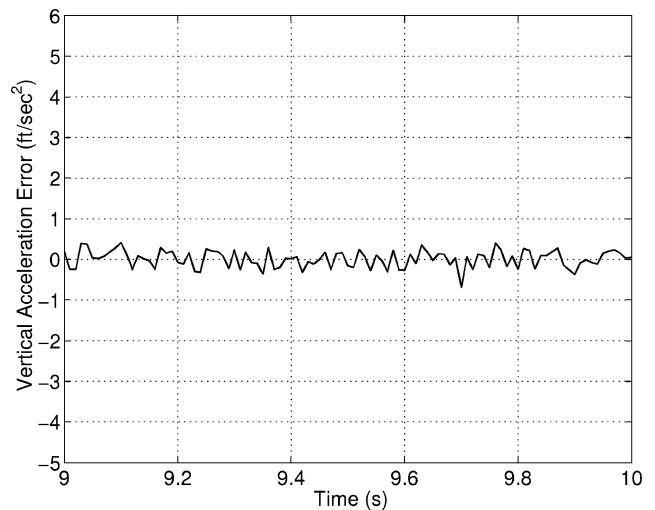
To visualize the improvement obtained using the Wiener model, Fig. 12a shows the predicted acceleration response obtained using only the identified linear model, that is,  $\hat{N}(\cdot) = 1$ , tuned with the GVT data noted in Table 2. It is evident that the estimated linear responses does not match the measured vertical acceleration GVT data accurately, as can be appreciated by looking at the vertical acceleration error signal in Fig. 12b and comparing it with the results of Fig. 10e. Then, the use of the nonlinear AE/ASE modeling approach to update production flutter analysis tools is totally justified.

**Table 2 F/A-18 AAW modal parameters identified from unmodeled vertical dynamics**

Mode	Natural frequency $f_i$ , Hz	Damping ratio $\zeta_i$
1	6.3079	$1.4143 \times 10^{-2}$
2	9.6777	$3.6278 \times 10^{-2}$
3	13.7698	$3.2878 \times 10^{-2}$
4	15.8485	$4.0317 \times 10^{-2}$
5	18.3387	$1.3807 \times 10^{-2}$
6	20.6243	$2.1379 \times 10^{-2}$

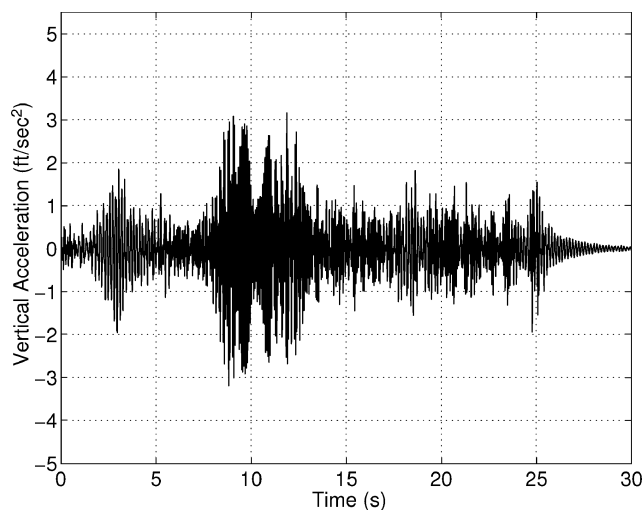


a) Vertical unmodeled acceleration responses between  $t_i = 9$  s and  $t_f = 10$  s

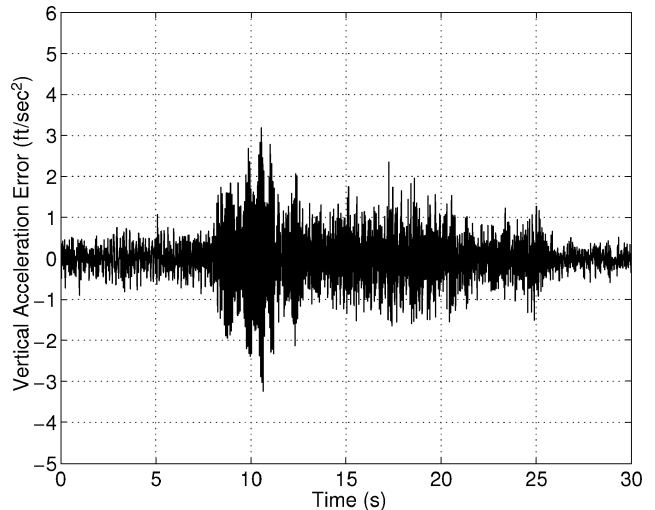


b) Vertical unmodeled acceleration error signal between  $t_i = 9$  s and  $t_f = 10$  s

**Fig. 11 F-18 AAW/GVT measured and identified vertical unmodeled acceleration data.**



a) Identified linear acceleration response



b) Vertical acceleration error signal

**Fig. 12 F-18 AAW/GVT vertical acceleration data.**

### Conclusions

In this paper, we consider a nonlinear AE/ASE modeling update by the identification of block-oriented models. Two different block-oriented models were considered by analyzing experimental data: the Hammerstein and Wiener models. The identification algorithms are noniterative and based on the LSE and SVD techniques.

The proposed approach sought to augment existing linear models with nonlinear operators derived by analyzing test data. Such an approach is warranted because current AE/ASE commercial packages are able to generate highly accurate representations of the linear dynamics. Thus, these models would be suitable for analyzing AE/ASE flight-test data if the unknown nonlinearities are included. Knowledge of the physics behind these nonlinearities is not yet mature so that using flight data to identify the nonlinearities is the best approach available.

This methodology is illustrated with simulated and experimental data. Additionally, a method is proposed to tune the set of orthonormal functions with the available AE/ASE information. The results obtained confirm that this model updating procedure reproduces the nonlinear dynamic behavior embedded in the observed experimental evidence with high accuracy. Furthermore, if the identified memoryless nonlinearity is an odd function, it can be replaced by its SIDF, and the resulting models could be used to compute robust stability margins using the  $\mu$  method that would identify both flutter and LCO instabilities regions of the flight envelope.

### Acknowledgments

Research is supported by NASA Dryden Flight Research Center under the Small Business Technology Transfer Phase I program. The first author thanks Juan Carlos Gómez at the Universidad Nacional de Rosario, Argentina, for his valuable discussions during the implementation of the block-oriented system identification technique.

### References

- <sup>1</sup>Prazenica, R. J., Brenner, M. J., and Lind, R., "Nonlinear Volterra Kernel Identification for the F/A-18 Active Aeroelastic Wing," International Forum on Aeroelasticity and Structural Dynamics, IFASD-US-32, Amsterdam, June 2003.
- <sup>2</sup>Brenner, M., and Prazenica, R. J., "Aeroservoelastic Model Validation and Test Data Analysis of the F/A-18 Active Aeroelastic Wing," International Forum on Aeroelasticity and Structural Dynamics, IFASD-US-32, Amsterdam, June 2003.
- <sup>3</sup>Bunton, R. W., and Denegri, C. M., Jr., "Limit Cycle Oscillation Characteristics of Fighter Aircraft," *Journal of Aircraft*, Vol. 37, No. 5, 2000, pp. 916–918.
- <sup>4</sup>Norton, W. J., "Limit Cycle Oscillation and Flight Flutter Testing," *Proceedings of the Society of Flight Test Engineers 21st Annual Symposium*, Paper 21-15, 1990.
- <sup>5</sup>Gómez, J. C., and Baeyens, E., "Identification of Nonlinear Systems Using Orthonormal Bases," *Proceedings of the IASTED International Conference on Intelligent Systems and Control*, ISC 2001, 2001, pp. 126–131.
- <sup>6</sup>ZAERO User's Manual, Ver. 7.1, ZONA Technology Inc., Scottsdale, AZ, URL: <http://www.zonatech.com> [cited Aug. 2004].
- <sup>7</sup>Ferreres, G., and Fromion, V., "Nonlinear Analysis in the Presence of Parametric Uncertainties," *International Journal of Control*, Vol. 69, No. 5, 1998, pp. 695–716.
- <sup>8</sup>Lind, R., Prazenica R. J., and Brenner, M. J., "Estimating Nonlinearity Using Volterra Kernels in Feedback with Linear Models," AIAA Paper 2003-1406, April 2003.
- <sup>9</sup>Baldelli, D. H., Lind, R., and Brenner, M., "Nonlinear Aeroelastic Modeling by Block-Oriented Identification," AIAA Paper 2004-1938, April 2004.
- <sup>10</sup>Smith, R., and Dullerud, G., "Modeling and Validation of Nonlinear Feedback Systems," *Robustness in Identification and Control*, edited by A. Garulli, A. Tesi, and A. Vicino, Springer-Verlag, London, 1999, pp. 87–101.
- <sup>11</sup>Bodin, P., Oliveira e Silva, T., and Wahlberg, B., "On the Construction of Orthonormal Basis Functions for System Identification," *13th Triennial World Congress, IFAC 1996*, pp. 369–374, 3a-12-3.
- <sup>12</sup>Golub, G. H., and Van Loan, C. F., *Matrix Computations*, 3rd ed., Johns Hopkins Univ. Press, Baltimore, MD, 1996.
- <sup>13</sup>Ko, J., Kurdila, A. J., and Strganac, T. W., "Nonlinear Control of a Prototypical Wing Section with Torsional Nonlinearity," *Journal of Guidance, Control, and Dynamics*, Vol. 20, No. 6, 1997, pp. 1181–1189.
- <sup>14</sup>Voracek, D., Pendleton, E., Reichenbach, E., Griffin, K., and Welch, L., "The Active Aeroelastic Wing Phase I Flight Research Through January 2003," NASA TM-2003-210741, May 2004.
- <sup>15</sup>Mignolet, M. P., and Red-Horse, J. R., "ARMAX Identification of Vibrating Structures: Model and Model Order Estimation," *Proceedings of the 35th AIAA/ASME/ASCE/AHS/ASC Structures, Structural Dynamics, and Materials Conference*, AIAA, Washington, DC, 1994, pp. 1628–1637.
- <sup>16</sup>Juang, J.-N., Cooper, J. E., and Wright, J. R., "An Eigensystem Realization Algorithm Using Data Correlations (ERA/DC) for Modal Parameter Identification," *Control Theory and Advance Technology*, Vol. 4, No. 1, 1988, pp. 5–14.
- <sup>17</sup>Vold, H., and Recklin, G. F., "The Numerical Implementation of a Multi-Input Modal Estimation Method for Mini Computers," *Proceedings of the International Modal Analysis Conference*, Nov. 1982.